STRUCTURAL CONCEPTS AND AERODYNAMIC DESIGN OF SHOCK CONTROL BUMPS

W. Wadehn, A. Sommerer, Th. Lutz, D. Fokin, G. Pritschow, S. Wagner
Institute for Control Engineering (ISW), Seidenstrasse 36, 70174 Stuttgart, Germany
Institute for Aerodynamics and Gas Dynamics, Pfaffenwaldring 21, 70550 Stuttgart, Germany

Keywords: *Adaptive Wing, Shock Control Bump, Shape Adaptive Systems, Optimisation*

Abstract

The design of adaptive structures for enhanced system performance in aircraft applications is a highly interdisciplinary topic. In this paper a combined design under consideration of the aerodynamic as well as the structural requirements of a shock control bump (SCB) is presented. Using a new parametrisation technique for the shape of the SCB, the aerodynamic optimisation is performed while at the same time producing an actuator optimal solution for each design. An actuation concept will be shown which is able to generate a bump with adaptable maximum position and height according to the current flight condition. A new control is presented which applies the optimal solution to an experimental demonstrator.

1 Introduction

Flight at transonic MACH numbers is characterised by the problem of emerging shock waves on the suction side of the wing causing the transonic drag rise. With new transport aircraft concepts aiming at higher flight MACH numbers measures must be taken to avoid the rapid increase of the drag coefficient when flying beyond the drag rise MACH number. One way to cope with that problem is the geometrical adaptation of the airfoil shape according to current flight conditions. By taking advantage of the highly nonlinear character of transonic flows, the region of the airfoil to be adapted can be restricted to a small zone. The adaptive mechanism investigated here is the so-called shock control bump proposed in 1992 by ASHILL ET. AL. [1]. Isentropic compression waves that emanate from the concave region of the upstream flank of the bump increase the pressure upstream of the shockwave thus reducing the shock strength. This leads to a lower loss of total pressure across the shock resulting in lower wave drag. Investigations conducted up to now [10, 20] including the numerical optimisation of several basic SCB shapes [18] and the combined application of an SCB with a variable camber mechanism [19] demonstrate the drag reduction potential.

The conventional structural concepts proposed so far could not meet all requirements because of the contradiction of structural stiffness required to counteract the aerodynamic forces and the flexibility needed to enable a geometric adaptation [5]. By using structure integrated actuation systems the new approach of adaptive structures aims on enhancing the capabilities of the structure to react on external loads or changing conditions. Since the principal design of the aircraft should not be modified, the adaptive SCB structure can be integrated in the wing spoilers. This enables a geometry adaptation in the vicinity of the shock without adding too much complexity and weight. For the generation of the active surface of the SCB several kinematic systems were compared [15]. Since there are severe requirements with respect to stiffness and safety, the functional structure of the proposed arrangement is separated from the supporting structure

through a mechanical parallel actuation system. This approach has very good capabilities for geometrical adaptation, but special attention has to be paid to the actuation of the structure since the system is mechanically overdetermined.

2 Tools for the Aerodynamic Design of SCBs

To investigate the aerodynamic drag reduction potential of SCBs numerical optimisations were performed. A modular optimisation environment was developed consisting of an optimiser, a geometry module and an aerodynamic analysis code [19, 18]. To increase efficiency, the code was implemented under the MPI parallel application interface [8]. A *pool-of-tasks* concept enables a uniform processor load even on heterogeneous parallel environments. The 2D Euler Code MSES [7] represents the analysis module in the optimisation environment. To account for viscous effects, it is coupled with an integral boundary layer method. MSES provides a robust as well as a highly efficient solution process. An optimisation algorithm based on an evolution strategy [16] was used. A coupled covariance matrix adaptation [9] provides an adjusted individual mutation stepsize.

3 Combined Design of a SCB

As shown in previous investigations [18], the aerodynamic effect of the bump is dominated by the global position of the SCB on the airfoil and the location of the bump maximum with height ζ and local maximum position ξ (Fig. 1). The detailed shape of the bump is of minor importance. Therefore, a the new set of parameters ν for the maximum of the SCB is introduced:

$$\nu = [\xi, \zeta] \tag{1}$$

Usually, the contour of a loaded beam or a polynomial is chosen to represent the SCB shape during the aerodynamic design. Here, an attempt is made to derive a family of SCB shapes [17] which account for the structural requirements of a system with distributed actuators (Fig. 1).

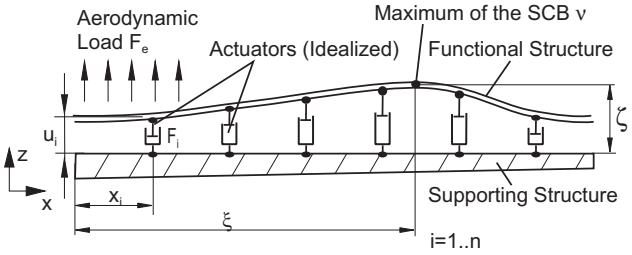

Fig. 1 Distributed Actuation System

As will be shown, with this procedure the actuator forces F_i required to obtain the corresponding SCB shape are fully determined by the parameters ζ and ξ. Thus, for the aerodynamic optimisation and the control design the system of n forces F_i is reduced to a system of two degrees of freedom.

The analytical model of the actuation system shown in Fig. 1 can be deduced according to eq. (2). The deformation z of the functional structure result form the general forces F_G acting on the system which can be separated in n controllable actuator forces F_i and the external forces F_e from the aerodynamic load. The actuator forces F_i are produced by the extension u_i of the actuators in direction p_i. The resulting equations are given by the structural stiffness K:

$$F_G = Ku \tag{2}$$

In principle the structural stiffness K could be derived from the Karman plate theory [2], but for the following 2D considerations with small deformations the linear theory of Euler-Bernoulli with a tangential boundary condition for the functional structure is used. Since the direction p_i of all actuators is normal to the supporting structure the equations can be very much simplified. The error in comparison to the nonlinear theory is less than 1% if the derivation of the bending line accounts less than $0.15 \ldots 0.20$ [3] but the computational effort is much lower.

At the location x_i of the actuator force F_i the displacement of a clamped beam with normalised length, modulus of elasticity and geo-

metrical moment of inertia is written as follows:

$$z_i = \underbrace{\frac{x_i^3(1-x_i^3)}{3}}_{a_i} \cdot F_i = a_i \cdot F_i \tag{3}$$

The optimal functional correlation between ν and the force parameters F_i is defined with respect to the needs of the actuators used. Stress sensitive actuators like shape memory actuators may focus on an absolute minimal stress in combination with minimal energy consumption whereas e. g. hydraulic actuators may merely focus on the actuator displacement and stress of the functional structure. As a compromise, for the following investigations the criterion of minimal deformation energy is used. According to the principle of superposition the deformation energy introduced due to n actuators amounts to:

$$E = \sum_{i=1}^{n} a_i F_i^2 \tag{4}$$

3.1 Derivation of a New SCB Shape Family

The energy term (4) is to be minimised under consideration of a number of constraints. A suitable method for the solution of such an isoperimetric problem is described by an extended Lagrangian-Multiplier method. Since there are not only equality constraints prescribed but also inequality conditions the Karush-Kuhn-Tucker theorem [11] must be introduced additionally. The displacement at the position of the bump-maximum $x = \xi$ caused by n actuator forces is:

$$z(\xi) = \sum_{i=1}^{n} b_i F_i \tag{5}$$

with

$$b_i = \frac{(1-x_i)^2}{6}\xi^2\Big[3x_i - (1+2x_i)\xi\Big] \tag{6}$$
$$\text{for all } x_i \geq \xi$$
$$b_i = \frac{(1-\xi)^2}{6}x_i^2\Big[3(1-x_i) - (1+2(1-x_i))(1-\xi)\Big] \tag{7}$$
$$\text{for all } x_i < \xi$$

The slope of the SCB contour at the position $x = \xi$ amounts to:

$$z'(\xi) = \sum_{i=1}^{n} c_i F_i \tag{8}$$

with

$$c_i = \frac{(1-x_i)^2}{2}\xi\Big[2x_i - (1+2x_i)\xi\Big] \tag{9}$$
$$\text{for all } x_i \geq \xi$$
$$c_i = -\frac{1-\xi}{2}x_i^2\Big[2(1-x_i) - (3-2x_i)(1-\xi)\Big] \tag{10}$$
$$\text{for all } x_i < \xi$$

The equality conditions that fix the height ζ and the position of the bump maximum ξ are:

$$\sum_{i=1}^{n} b_i F_i = B \qquad \text{with} \quad B = \zeta \tag{11}$$

$$\sum_{i=1}^{n} c_i F_i = C \qquad \text{with} \quad C = 0 \tag{12}$$

The inequality constraints that prevent negative ordinate values of the contour at the positions of the actuators are written as follows:

$$\begin{aligned} \sum_{j=1}^{n} d_{1j} F_j &\geq D_1 \\ &\vdots \\ \sum_{j=1}^{n} d_{nj} F_j &\geq D_n \end{aligned} \tag{13}$$

with

$$d_{ij} = \frac{(1-x_j)^2}{6}x_i^2\Big[3x_j - (1+2x_j)x_i\Big] \tag{14}$$
$$\text{for all } x_j \geq x_i$$
$$d_{ij} = \frac{(1-x_i)^2}{6}x_j^2\Big[3(1-x_j) - (3+2(1-x_j))(1-x_i)\Big] \tag{15}$$
$$\text{for all } x_j < x_i$$

and

$$D_1, \ldots, D_n = 0 \tag{16}$$

According to [11] the function to be minimised contains the Lagrangian multipliers λ_1, λ_2 as well as the Karush-Kuhn-Tucker multipliers $\mu_1, \ldots, \mu_n$.

$$I(F_1,\ldots,F_n,\lambda_1,\lambda_2,\mu_1,\ldots,\mu_n) = \sum_{i=1}^{n} a_i F_i^2 + \lambda_1\left(\sum_{i=1}^{n} b_i F_i - B\right) + \lambda_2\left(\sum_{i=1}^{n} c_i F_i - C\right) + \mu_1\left(\sum_{j=1}^{n} d_{1j} F_j - D_1\right) + \ldots + \mu_n\left(\sum_{j=1}^{n} d_{nj} F_j - D_n\right) \tag{17}$$

To determine the values of λ_1, λ_2 the partial derivatives for the n forces are calculated:

$$F_s = -\lambda_1 \frac{b_s}{2a_s} - \lambda_2 \frac{c_s}{2a_s} - \sum_{k=1}^{n} \mu_k \frac{d_{ks}}{2a_s} \tag{18}$$
$$\text{for} \quad s = 1,\ldots,n$$

Inserting (18) into (11) and (12) leads to a 2x2 linear equation system with the parameters μ_k still unknown. By applying Cramer's rule [4] the Lagrangian multipliers become:

$$\lambda_1 = \frac{-Ba_{22} + Ca_{12}}{D} + \sum_{k=1}^{n} \mu_k \frac{-B_k a_{22} + C_k a_{12}}{D} \tag{19}$$

$$\lambda_2 = \frac{-Ca_{11} + Ba_{12}}{D} + \sum_{k=1}^{n} \mu_k \frac{-C_k a_{11} + B_k a_{12}}{D} \tag{20}$$

with

$$B_k = \sum_{s=1}^{n} \frac{b_s d_{ks}}{2a_s} \qquad C_k = \sum_{s=1}^{n} \frac{c_s d_{ks}}{2a_s} \tag{21}$$

Inserting (19) and (20) into (18) an equation forms that provides the optimum actuator forces F_s:

$$\begin{aligned} F_s = {} & \frac{b_s}{2a_s}\left[\frac{Ba_{22} - Ca_{12}}{D} - \sum_{k=1}^{n} \mu_k \frac{-B_k a_{22} + C_k a_{12}}{D}\right] \\ & + \frac{c_s}{2a_s}\left[\frac{Ca_{11} - Ba_{12}}{D} - \sum_{k=1}^{n} \mu_k \frac{-C_k a_{11} + B_k a_{12}}{D}\right] \\ & - \sum_{k=1}^{n} \mu_k \frac{d_{ks}}{2a_s} \\ = {} & \underbrace{\left[\frac{Ba_{22} - Ca_{12}}{2a_s D} b_s + \frac{Ca_{11} - Ba_{12}}{2a_s D} c_s\right]}_{P_s} \\ & + \sum_{k=1}^{n} \mu_k \left[\frac{B_k a_{22} - C_k a_{12}}{2a_s D} b_s \right. \\ & \left. + \frac{C_k a_{11} - Ba_{12}}{2a_s D} c_s - \frac{d_{ks}}{2a_s}\right] \end{aligned} \tag{22}$$

$$\rightarrow F_s = P_s + \sum_{k=1}^{n} \mu_k \cdot Q_{sk} \tag{23}$$

The parameters μ_k are fixed by the inequality conditions (13):

$$\sum_{s=1}^{n} d_{ls}\left[P_s + \sum_{k=1}^{n} \mu_k Q_{sk}\right] \geq D_l$$

$$\underbrace{\sum_{s=1}^{n} d_{ls} P_s}_{\tilde{P}_l} + \sum_{k=1}^{n} \mu_k \underbrace{\left[\sum_{s=1}^{n} d_{ls} Q_{sk}\right]}_{\tilde{Q}_{lk}} \geq D_l$$

$$\sum_{k=1}^{n} \mu_k \cdot \tilde{Q}_{lk} \geq D_l - \tilde{P}_l \tag{24}$$
$$\text{for} \quad l = 1,\ldots,n$$

The inequality system is transformed into a linear equation system by the following rule according to the Karush-Kuhn-Tucker theorem:

$$\text{If} \quad D_l - \tilde{P}_l \leq 0 \qquad \mu_l = 0 \tag{25}$$

$$\text{If} \quad D_l - \tilde{P}_l > 0 \qquad \text{RHS} = D_l - \tilde{P}_l \tag{26}$$

The values of μ_k are determined by a LU-decomposition followed by a forward / backward substitution. Inserting the μ_k into eq. (23) the values of the actuator forces F_s can be calculated.

Fig. 2 shows an actuator optimal contour with $\zeta = 0.005$ and $\xi = 0.7$. The actual forces acting on the functional structure (black bars) result from the superposition of the actuator forces

(grey bar) and the inner forces caused by prestress.

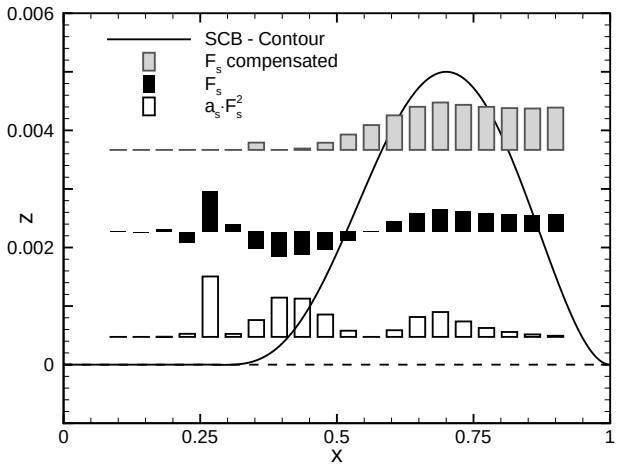

Fig. 2 Actuator forces and bending line for a SCB with $\zeta = 0.005$ and $xi = 0.7$ [17]

Furthermore, the comparison of the minimal energy consumption criterion with other objective functions like the maximum force criterion shows that there is only a slight difference in the distribution of the forces between all objective functions which utilise force terms by a power of greater than 1. The resulting shapes turn out to be quite similar as well.

3.2 Drag Reduction Potential of the Actuator Optimum SCB

In this section it is shown that the low-dimensional parametrisation technique described above yields almost the same aerodynamic drag reduction potential as a higher DOF polynomial SCB shape. Two optimisations were performed for a transonic DA VA2 airfoil at $M = 0.765$, $c_l = 0.524$ and $Re = 1 \cdot 10^7$ [17]. The optimised polynomial bump of the basic parametrisation

$$z(x) = \sum_{i=0}^{11} a_i \cdot x_i \qquad (27)$$

with 8 DOF leads to an overall drag reduction of 15% while the actuator optimal SCB described above yields 14% (Fig. 3).

These results confirm the assumption that the aerodynamic optimisation towards drag reduction is not hampered by the additional considera-

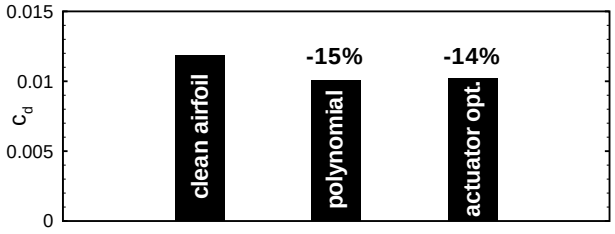

Fig. 3 Possible drag reductions for different parametrisations, DA VA2 airfoil, $M = 0.765$, $c_l = 0.524$, $Re = 1 \cdot 10^7$

tion of constraints introduced by a potential actuator system.

4 Proposed Structural Concept

In the considerations above the system is represented by idealised forces and bending lines. In the real application the bending line must be generated by available actuators and a kinematic structure. Therefore, possible combinations were compared [15]. In order to create a lightweight system, a prestressed moonie kinematics in combination with shape memory actuators was suggested. The kinematics fulfils several tasks [6]:

- It provides a mechanical parallel support of the functional structure
- It redirects the in-plane contraction to an out-plane motion
- It transmits the motion of the actuator to an extension of $\Delta h/h > 100\%$
- It creates an elasticity for the unidirectional actuators.

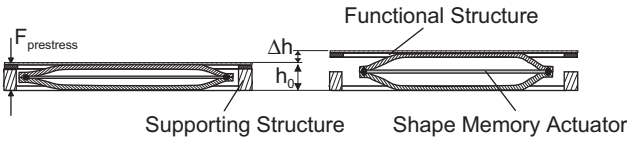

Fig. 4 Kinematics of the proposed system

The inner forces caused by the prestress of the kinematics have the following effects [15]:

- The inner forces generate an offset force which enhances unidirectional actuators to apply negative forces on the functional structure.

- The active forces needed could be reduced by a system with nonlinear stiffness.

The motion is generated by shape memory actuators. They produce high stresses (up to $200\,\mathrm{N/mm^2}$) in combination with relatively large strains (up to 3.5%) and could be minimised to the size needed. An actuation system with enhanced bandwidth and moderate currents could be obtained by the use of a mechanical parallel and electrical serial multi-actuator system [14]. In comparison to a single actuator element the increase of the electrical resistivity of an actuator element with n electrical serial sections is given by:

$$\frac{R_n}{R_0} = \frac{\rho A_n L_n}{\rho A_0 L_0} = n^2 \tag{28}$$

The increase in the dynamics can be calculated by the dominating heat convection:

$$Q_{\mathrm{conv}} = \alpha \cdot A \cdot (\vartheta_\infty - \vartheta_{\mathrm{actuator}}) \tag{29}$$

The characteristic heat transfer ratio α can be calculated by similarity considerations using the Nusselt ratio [21]. An approximation of the heat transfer ratio α depending on the number of mechanical parallel sections and the bandwidth gained is described by:

$$\alpha = 0.167 \cdot \lambda \left(\frac{Pr(\vartheta_{\mathrm{Aktor}} - \vartheta)}{\nu^2 d_a} \right)^{1/4} \tag{30}$$

The evaluation of eqs. (29) and (30) with mean values for λ, Pr and ν leads to a dependency as shown in Fig. 5. The parallel actuator element, used for the experimental realisation consists of $n = 10$ wires of a diameter of $0.38\,\mathrm{mm}$ which results in a resistance of $9.4\,\Omega$ and a bandwidth of about $0.3\,\mathrm{Hz}$.

The sensor information of the demonstrator is gained by absolute and relative position sensors along with force sensors located at each actuator (see Fig. 6).

5 Control Concept

To generate a controlled shape adaptation according to the desired values, the actuators G_P have

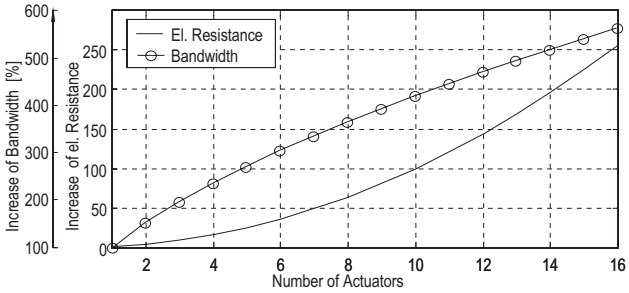

Fig. 5 Improvement of a multi-actuator system

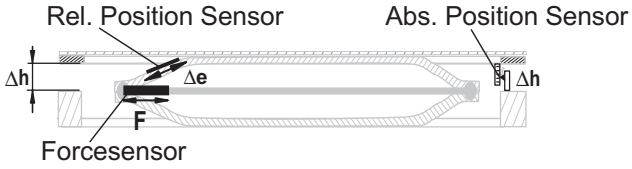

Fig. 6 Proposed sensor systems

to be heated in a closed control loop. One special aspect of using solid state actuators working in parallel which also have a load carrying function is that the control device has to consider structural issues additionally. Therefore, a *structure sensitive* controller was developed which is divided in n inner SISO single Actuator Control Loops ($G_{\mathrm{ACL},i}$) and an outer MIMO Sensor Control Loop (G_{SCL}) [12]. The structure of the control concept is depicted in Fig. 7. For the sake of simplicity the Laplace variable s is omitted in the block diagrams.

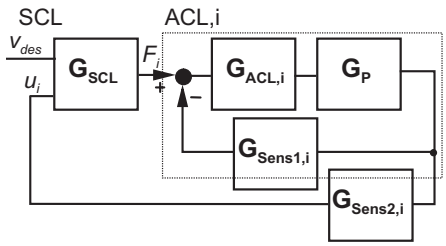

Fig. 7 Block diagram of the Control

The ACL works on the basis of the directly measured actuator forces $G_{\mathrm{Sens1},i}$ and is implemented by robust PI-controllers with the following transfer function:

$$G_{\mathrm{ACL},i} = K_p \left(1 + \frac{1}{T_n \cdot s} \right) \tag{31}$$

One issue of shape memory actuators is the long dead time at the beginning of the phase

transformation. Therefore an Anti-Windup-Algorithm has to be implemented:

$$T_n \to \infty \quad \text{if} \quad \dot{\nu}_{\text{des}} \neq 0 \tag{32}$$

Furthermore, the stress on the structure and actuators can be reduced by limiting the maximum contraction rate $\dot{\varepsilon}$ for the stress induced martensite generation (eq. (33)) and an adaptation of the control parameters if the structure overshoots its desired shape (34):

$$K_p \to 0 \quad \text{if} \quad \dot{\varepsilon} \geq \dot{\varepsilon}_{\max} \tag{33}$$

$$T_n \to 0 \quad \text{if} \quad u_i > u_{i,\text{des}} \tag{34}$$

The main task of the SCL controller is to regulate the exact shape and concurrently the optimal distribution of the actuator forces F_i. The objective function used will be named G_{OF} and is a general term of u_i and F_i :

$$G_{\text{OF}} = f(u_i, F_i) \tag{35}$$

For the further discussion of the SCL the variables G_{ACL}, G_P and G_{Sens1} will be merged to H_{ACL}:

$$H_{\text{ACL},i} = \frac{G_{\text{ACL},i} \cdot G_P}{1 + G_{\text{ACL},i} \cdot G_P \cdot G_{\text{Sens1},i}} \tag{36}$$

The calculation of the global maximum given by (1) from the local displacements of the actuators u is done by means of the transformation $T_{u\nu}$:

$$\nu = T_{u\nu} u \tag{37}$$

A closed solution of $T_{u\nu}$ can be implemented by a normalised polynomial approximation $(x_{i-1} = -1, x_i = 0, x_{i+1} = 1)$.

$$\xi = \frac{u_{i-1} - u_{i+1}}{2(u_{i-1} - 2u_i + u_{i+1})} \tag{38}$$

$$\zeta = -\frac{u_{i-1}^2 + 16u_i^2 + u_{i+1}^2 - 8u_{i-1}u_i}{8(u_{i-1} - 2u_i + u_{i+1})} - \frac{-2u_{i-1}u_{i+1} - 8u_i u_{i+1}}{8(u_{i-1} - 2u_i + u_{i+1})} \tag{39}$$

The SCL can be implemented as an online or offline optimisation controller:

The *offline optimisation* control uses precalculated values of a model of the structure. With the model of eq. (2) and the objective function described by eq. (23) the optimal forces of the actuation system for a given shape are predetermined and stored in a lookup table $T_{\nu f}$. In order to eliminate deviations caused by external forces and deviations of the model the input values of the transformation $T_{\nu f}$ will be adjusted by the PI control algorithm G_{Opt}.

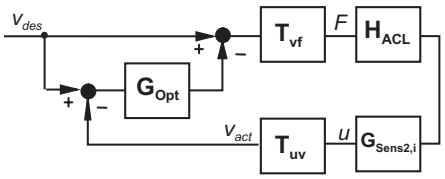

Fig. 8 Block diagram of the off-line SCL-controller

The advantages of the offline SCL-Controller are higher adjustable control parameters and the greater robustness against errors. However, the individual forces F_i show a greater deviation compared to the theoretical optimum.

The *online optimisation* control needs no model of the plant since in every time step the forces will be adjusted due to the input of the PI control algorithm G_{Opt} which has the input of the weighted signal from the deviation of ν according to eq. (37) with gain K_ν and the signal from the objective function G_{OF} with gain K_O. Since there is a strong mechanical coupling between the single actuation systems, they will adapt their height due to the exact maximum position by the upper branch of the weighting function ($K_{\nu,i}$) and try to optimise their force due to the lower branch (K_O). Fig. 9 illustrates the concept of the controller.

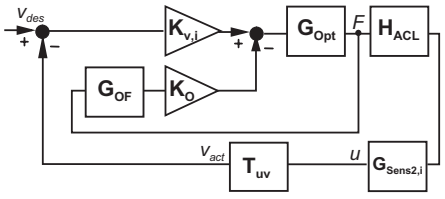

Fig. 9 Block diagram of the online SCL-controller

The online optimisation has the benefit of a very precise adaptation of the forces because no

model of the structure is used but on the other hand only lower control parameters are possible.

6 Demonstrator of an Adaptive Spoiler

The proposed combined design and control concept was tested in a model of an adaptive spoiler which is manufactured as a sandwich structure with integrated moonie kinematics actuated by shape memory actuators. The bottom side is depicted in Fig. 10. The sensors used are absolute position and force sensors in the mounting of the actuator elements.

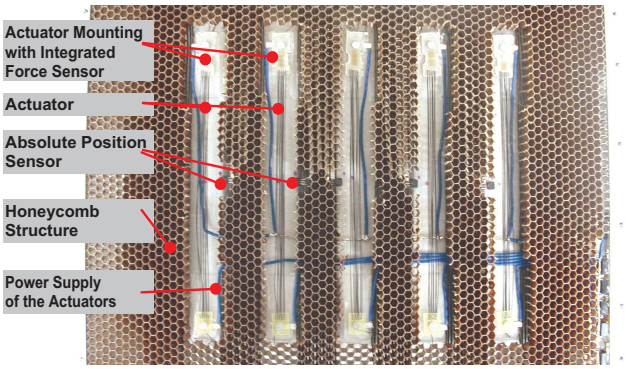

Fig. 10 Model of an adaptive spoiler

For the experimental comparison of the control structures Fig. 11 shows the measured actuator forces for a SCB shape with position controlled ACLs according to the force optimised position values. Actuator 2 has obviously the lowest dead time and applies a great force to generate the bump. After a while the remaining actuators follow which results in a better distribution of the load. However, an optimal distribution of the forces is not achieved due to manufacturing inaccuracies and external forces even if the optimal shape is gained.

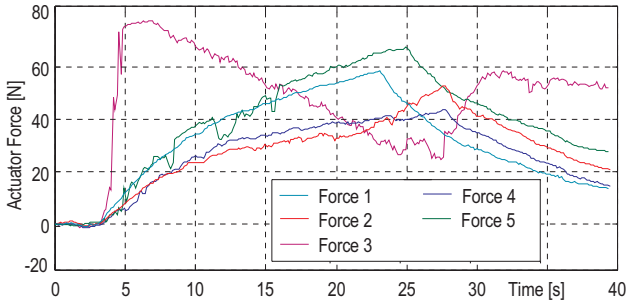

Fig. 11 Actuator forces without force control

The applied force control with force optimisation in centred position is shown in Fig. 12. During every time step the force of each actuator is adapted according to a maximum force criterion through the inner branch G_{OF} of Fig. 9. In the shown centre position all actuator forces feature the same value.

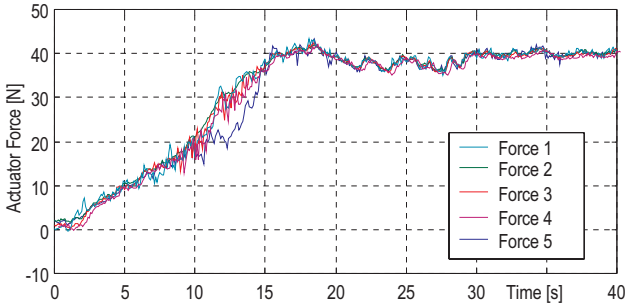

Fig. 12 Actuator forces with force control

The comparison of the bending lines of both controls show no visible difference. This means that the effect on the bending lines caused by unevenly distributed forces are so small that it can not be detected by position sensors.

7 Conclusion

In this paper, a new design approach for an adaptive SCB was introduced which considers both aerodynamic and structural requirements and leads to systems with minimised actuator forces and deformation energy. By means of analytical optimisation this approach inherently produces an actuator optimal SCB contour for a given height and position of the SCB maximum.

With the application of a numerical optimisation scheme it was shown that the drag reduction potential of a SCB is not hampered by the introduction of the proposed basic shape parametrisation. The possible drag reduction is comparable to that of a higher order polynomial contour approach.

A structural concept for an adaptive spoiler was developed which utilises a moonie actuation system in combination with shape memory alloys. A "structural sensitive" controller was developed which consists of a sensor control loop for exact position control and cascaded actuator

control loops for the even distribution of the actuator forces. To prove the proposed concepts a small scale demonstrator was built. This adaptive SCB showed the desirable geometric accuracy and a great robustness against external disturbances. The actuator forces are only moderate so that long term durability of the actuators can be anticipated.

8 Acknowledgements

The authors thank M. Drela of the MIT for providing MSES that is part of the present optimisation environment. This research project is funded by the Ministry for Science, Research and Art in Baden-Württemberg as well as the German Research Foundation (DFG).

References

[1] P. R. Ashill, J. L. Fulker, and A. Shires. A novel technique for controlling shock strength of laminar-flow aerofoil sections. In *Proceedings 1st European Forum on Laminar Flow Technology, March 16–18, 1992, Hamburg, Germany*, pages 175–183. DGLR, AAAF, RAeS, 1992.

[2] T. Bein, H. Hanselka, and E. Breitbach. The adaptive spoiler - mechanical aspects of a local spoiler thickening to control the transonic shock. In *Proceedings of the 9th International Conference on Adaptive Structures and Techniques*, 1998.

[3] W. Brand, C. Boller, M. S. Huang, and L. C. Brinson. Introducing the constitutive behaviour of shape memory alloy into adaptive engineering structures. In *Proceedings of the ASME Winter Annual Meeting: Symposium on the Mechanics of Phase Transformation and Shape Memory Alloys, 1994, Chicago, USA*, 1994.

[4] I. N. Bronstein and K. A. Semendjajew. *Taschenbuch der Mathematik*. Verlag Nauka, Moskau; B. G. Teubner Verlagsgesellschaft, Stuttgart/Leipzig; Verlag Harri Deutsch, Thun und Frankfurt/Main, 25 edition, 1991.

[5] L. F. Campanile and D. Sachau. Distributed versus concentrated flexibility in shape control of lifting surfaces: The belt-rib structural concept. In *Proceedings of the ASME Design Engineering Technical Conference, 1999, Las Vegas, USA*, 1999.

[6] L. F. Campanile, D. Sachau, and S. Seelecke. Ein adaptives Windkanalmodell für einen adaptiven Tragflügel. Technical report, DGLR, 1999. DGLR-Paper No. JT99-050.

[7] M. Drela. Design and optimization method for multi-element airfoils. In *Aerospace Design Conference*, Irvine, CA, USA, February 1993. AIAA / AHS / ASEE.

[8] M. P. Forum. *MPI-2: Extensions to the Message Passing Interface*. NSF and DARPA, July 1997. NSF contract CDA-9115428.

[9] N. Hansen. *Verallgemeinerte individuelle Schrittweitenregelung in der Evolutionsstrategie: Eine Untersuchung zur entstochastisierten, koordinatensystemunabhängigen Adaption der Mutationsverteilung*. Dissertation, Technische Universität Berlin, 1998. Veröffentlicht im Mensch & Buch Verlag, Berlin. ISBN 3-933346-29-0, 1998.

[10] A. Knauer. *Die Leistungsverbesserung transsonischer Profile durch Konturmodifikationen im Stossbereich*. PhD thesis, DLR, 1998.

[11] A. L. Peressini, F. E. Sullivan, and J. J. Uhl. *The Mathematics of Nonlinear Programming*. Springer Verlag, Berlin Heidelberg New York, 1988. ISBN 0-387-96614-5 & ISBN 3-540-96614-5.

[12] G. Pritschow and W. Wadehn. Regelkonzepte für formadaptive Struktursysteme. In *Proceedings of the 4th VDI Mechatronik Conference: Innovative Produktentwicklung, 12–13 September 2001, Frankenthal, Germany*, 2001.

[13] G. Pritschow and W. Wadehn. Sensor systems in shape adaptive structures for smart airfoils. In *Proceedings of the IEEE-Fachtagung: International Conference on Multisensor Fusion and Integration for Intelligent Systems, 20–22 August, 2001, Baden-Baden, Germany*, 2001.

[14] G. Pritschow and W. Wadehn. Design of an adaptive windtunnel mockup with shape memory alloys. In *Proceedings of the 8th International Conference on New Actuators, Actuator 2002, 10–12 June 2002, Bremen, Germany*, 2002.

[15] G. Pritschow, W. Wadehn, and G. Kehl. Shape

adaptation of fixed wing aircraft by shape memory alloys. In *Proceedings of the 7th International Conference on New Actuators, Actuator 2000, 10–12 June, 2000, Bremen, Germany*, 2000.

[16] I. Rechenberg. *Evolutionsstrategie '94 — Werkstatt Bionik und Evolutionstechnik, Band 1*. Frommann-Holzboog Verlag, Stuttgart, 1994. ISBN 3772816428.

[17] A. Sommerer and D. Fokin. Eine aktoroptimale Parametrisierung zur Erzeugung von Geometrien für Shock Control Bumps. Technical report, IAG, University of Stuttgart, 2002.

[18] A. Sommerer, T. Lutz, and S. Wagner. Design of adaptive transonic airfoils by means of numerical optimisation. In *Proceedings of ECCOMAS 2000, European Congress on Computational Methods in Applied Sciences and Engineering, 11–14 September, 2000, Barcelona, Spain*, 2000.

[19] A. Sommerer, T. Lutz, and S. Wagner. Numerical optimisation of adaptive transonic airfoils with variable camber. In *Proceedings of the 22nd International Congress of the Aeronautical Sciences, 27 August – 1 September, 2000, Harrogate, UK*, 2000.

[20] E. Stanewsky. Euroshock II and II: A survey. In G. E. A. Meier and P. R. Viswanath, editors, *Proceedings IUTAM Symposium on Mechanics of Passive and Active Flow Control, 7–11 September, 1998, Göttingen, Germany*, pages 35–42. Kluwer Academic Publishers, 1998.

[21] W. Wagner. *Wärmeübertragung*. Vogel Verlag, 2nd edition, 1998.